

07.3;08.3

InGaAlAs/InAlAs heterostructures for electro–absorption modulator

© D.V. Gulyaev, D.A. Kolosovsky, D.V. Dmitriev, A.K. Gutakovskii, E.A. Kolosovsky, K.S. Zhuravlev

Rzhanov Institute of Semiconductor Physics, Siberian Branch, Russian Academy of Sciences, Novosibirsk, Russia

E-mail: gulyaev@isp.nsc.ru

Received March 29, 2022

Revised May 5, 2022

Accepted May 17, 2022

The structural and optical characteristics of heterostructures with InGaAlAs/InAlAs quantum wells, in which a quaternary alloy is obtained by alternating monolayer growth of InAlAs and InGaAs layers by molecular beam epitaxy, have been investigated. It has been shown that obtained heterostructures are promising for creation of electro–absorption modulators designed for a wavelength of $1.55\ \mu\text{m}$ with the extinction coefficient of more than 20 dB at a voltage of less than 4 V.

Keywords: Electro–absorption modulator, molecular beam epitaxy, quantum wells, Stark effect.

DOI: 10.21883/TPL.2022.07.54034.19205

The modern trend for the development of systems for fiber–optic communication and radiophotonics (microwave photonics) stipulates the transition from the discrete element base to integrated circuits [1,2] that can be created only based on InP. The electro–absorption modulator (EAM) that is one of the key components of such circuits is to ensure minimum optical losses in the absence of bias and strong absorption at a small bias. For the wavelength of $1.55\ \mu\text{m}$, which is the case of minimal optical signal attenuation in optical fiber, EAM may be constructed based on heteroepitaxial structures (HESs) with InGaAlAs/InAlAs [3–5] or InGaAsP/InP [5–7] quantum wells (QWs). The InGaAlAs/InAlAs–based HESs are preferable since they ensure higher localization of excitons in QWs due to a larger band discontinuity and, hence, higher temperature stability and reduction of saturation effects [5,8]. The use of the quaternary InGaAlAs compound as the QW material enables shifting the QW absorption spectrum from the operating EAM wavelength ($1.55\ \mu\text{m}$) to the shortwave spectrum region due to broadening the band gap by increasing the Al fraction, as well as reducing the light absorption losses in the absence of bias. The technique, in which for this purpose only the quantum–size effect in the InGaAs QW is used, is hardly applicable since the QW width reduction necessary to shift the absorption spectrum is accompanied by a decrease in the magnitude of the Stark quantum–size effect [9]. At the same time, in the quaternary solid solutions there can occur spinodal decomposition [10] that does not exist in ternary compounds InGaAs and InAlAs [11,12]. A promising way of preventing such a decomposition of the InGaAlAs compounds is digital epitaxy [13] performed by alternating submonolayer and monolayer growth of the InGaAs and InAlAs ternary components of the InGaAlAs quaternary solid solutions. The quaternary solution composition is defined by the growth time (thickness) of the InGaAs and InAlAs sublayers. Among the advantages of this method there is a possibility of growing different–composition structures by using within

the molecular–beam epitaxy setup only a single set of initial material sources (In, Ga, Al and As). Ternary components InGaAs and InAlAs are grown by alternating opening/closing the Ga/Al sources. This technique does not need varying the source temperatures, which provides for good reproducibility and stability of specified compositions, namely, the In/Ga and In/Al ratios. At the same time, the optical and energetic properties of the homogeneous and digital InGaAlAs quaternary solutions may be different. In this work, structural and optical properties of HESs with the InGaAlAs/InAlAs QWs obtained by digital epitaxy were studied, and their perspectiveness for creating EAM with the $1.55\ \mu\text{m}$ wavelength was demonstrated.

The heterostructures were grown by molecular–beam epitaxy on an undoped InP (001) substrate at the Riber Compact-21T setup. Elemental composition of the InGaAlAs QWs in HES was varied. To precisely vary the QW composition and, hence, the band gap width, the ratio between the thickness of the $\text{In}_{0.52}\text{Al}_{0.48}\text{As}$ layer (two monolayers in all the studied samples) and that of the $\text{In}_{0.53}\text{Ga}_{0.47}\text{As}$ layer (six or eight monolayers in different samples). The studied HESs were $p-i-n$ -structures containing the following layers: 1) An InGaAs p^+ -layer 100 nm thick with the doping level of $1.5 \cdot 10^{19}\ \text{cm}^{-3}$ which is designed to protect the surface against oxidation; 2) the top (p^+ -InAlAs) and bottom (n^+ -InAlAs) contact layers 200 nm thick with the doping level of $5 \cdot 10^{18}\ \text{cm}^{-3}$; 3) additional n and p InAlAs layers 200 nm thick with the doping level of $5 \cdot 10^{16}\ \text{cm}^{-3}$ which ensure a linear decrease in voltage in the HES undoped region; 4) the HES central active region 300 nm thick consisting of multiple quantum wells (MQWs), namely, of 12 periods of the InGaAlAs/InAlAs MQWs 14/10 nm thick or 11 periods of MQWs 17/10 nm thick. The InAlAs barrier layers were grown at the temperature of $510\text{--}520^\circ\text{C}$ that is optimal for growing Al–containing layers; the InGaAlAs QWs were grown at $480\text{--}490^\circ\text{C}$. The temperature was changed at the initial and final stages of the InAlAs barrier layer growth, which corresponded to about

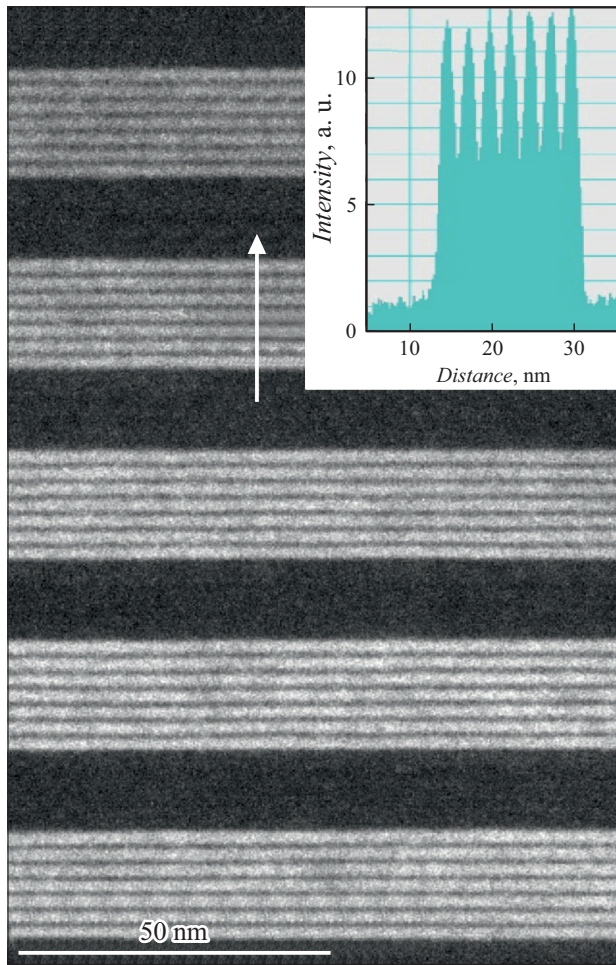


Figure 1. TEM image of a typical digital InGaAlAs/InAlAs QW. The inset presents a profile of the TEM image intensity distribution corresponding to the region marked with the arrow.

2 nm. As the acceptor dopant, Be was used; the donor dopant was Si. For studying electro-optical characteristics, test samples with ohmic contacts were prepared based on the $p-i-n$ structures. To form the bottom contact to n^+ -InAlAs, the Ge/Au/Ni/Au composition 20/40/20/200 nm thick was used; the top contact to p^+ -InGaAs was formed by using the Ti/Au composition 20/200 nm thick. The mesa lateral surface was covered by a SiO₂ layer 100 nm thick.

Fig. 1 presents a typical image of the active region of HES consisting of MQWs, which was obtained by transmission electron microscopy (TEM) in the cross-section mode (with microscope TITAN 80-300 having lateral resolution of 0.79 Å). As the figure shows, heteroboundaries of ternary solution layers used to form the InGaAlAs QWs are quite sharp. Intermixing of the InGaAs and InAlAs ternary solutions down to the homogeneous InGaAlAs solution is not observed even when InAlAs layers two monolayers in thickness are used, namely, the grown InGaAlAs QW itself is a short-period superlattice (see the Fig. 1 inset).

One can see from the HES photoluminescence (PL) spectra presented in Fig. 2, *a* that the band gap of MQW

with the ratio between monolayers InAlAs/InGaAs of 2/6 differs from the EAM operating wavelength by 0.21 μm; the same difference for MQW with the ratio of 2/6 is 0.15 μm. Full width at half maximum (FWHM) of the MQW PL band is 12–18 meV at the nitrogen temperature when FWHM is defined mainly by fluctuations of the well composition and thickness rather than by the temperature expansion. The measured PL band width is typical of the InGaAlAs/InAlAs MQW [14,15] and is relevant to the composition fluctuations within 1–2%.

To determine passive optical losses in MQWs, i.e. in the absence of bias, the reflection $R(\lambda)$ and transmission $T(\lambda)$ spectra of HESs consisting only of MQWs were measured using Fourier spectrometer Bruker vertex 80v. The absorption coefficient was defined as $\alpha(\lambda) = -\ln(1 - T(\lambda) - R(\lambda))/W$ (where W is the MQW total width), while passive optical losses were defined as $10 \lg(\exp(-\alpha(\lambda)L)) = -10 \lg e \alpha(\lambda)L$. As Fig. 2, *b* shows, passive losses in the studied MQWs do not exceed 1 dB/mm at 1.55 μm.

We have made calculations and compared the energy structures and charge carrier wave functions for the uniform and digital InGaAlAs QWs. The calculations were carried out using a test version of program code nextnano [16] that self-consistently solves the Poisson and Schrodinger equations. Figs. 3, *a, b* show that the charge carrier wave functions for the uniform and digital QWs differ only slightly since two monolayers of InAlAs are not a sufficient barrier for charge carriers.

The voltage dependence of extinction coefficient of the studied HES is illustrated in Fig. 3, *c*. The inset to this figure presents the geometry of the experiment in which light transmission across HES at the wavelength of 1.55 μm corresponding to the light wave TE mode was measured. In EAM, the light wave propagates along HES, i.e. its effect may be based on both the TE and TM light wave modes. Extinction coefficients of the light wave TE and TM modes differ from each other; however, in the first approximation they may be assumed to be equal [8]. The HES extinction coefficient is related to variations in absorption coefficient $\Delta\alpha(V)$ by the following formula:

$$T(V) = 10 \lg \left(\frac{I(V)}{I(0)} \right) \approx 10 \lg(\exp(-\Delta\alpha(V)L)),$$

where $I(0)$ and $I(V)$ are the intensities of light transmitted through HES in the absence/presence of electric field, V is the applied voltage, L is the EAM length. Since

$$\begin{aligned} \Delta I(V) &= \frac{I(0) - I(V)}{I(0)} \\ &\approx \frac{I_0 [\exp(-\alpha W) - \exp(-(\alpha + \Delta\alpha(V))W)]}{I_0 \exp(-\alpha W)} \\ &= 1 - \exp(-\Delta\alpha(V)W), \end{aligned}$$

obtain

$$\Delta\alpha(V) = -\ln(1 - \Delta I(V))/W \approx \Delta I(V)/W$$

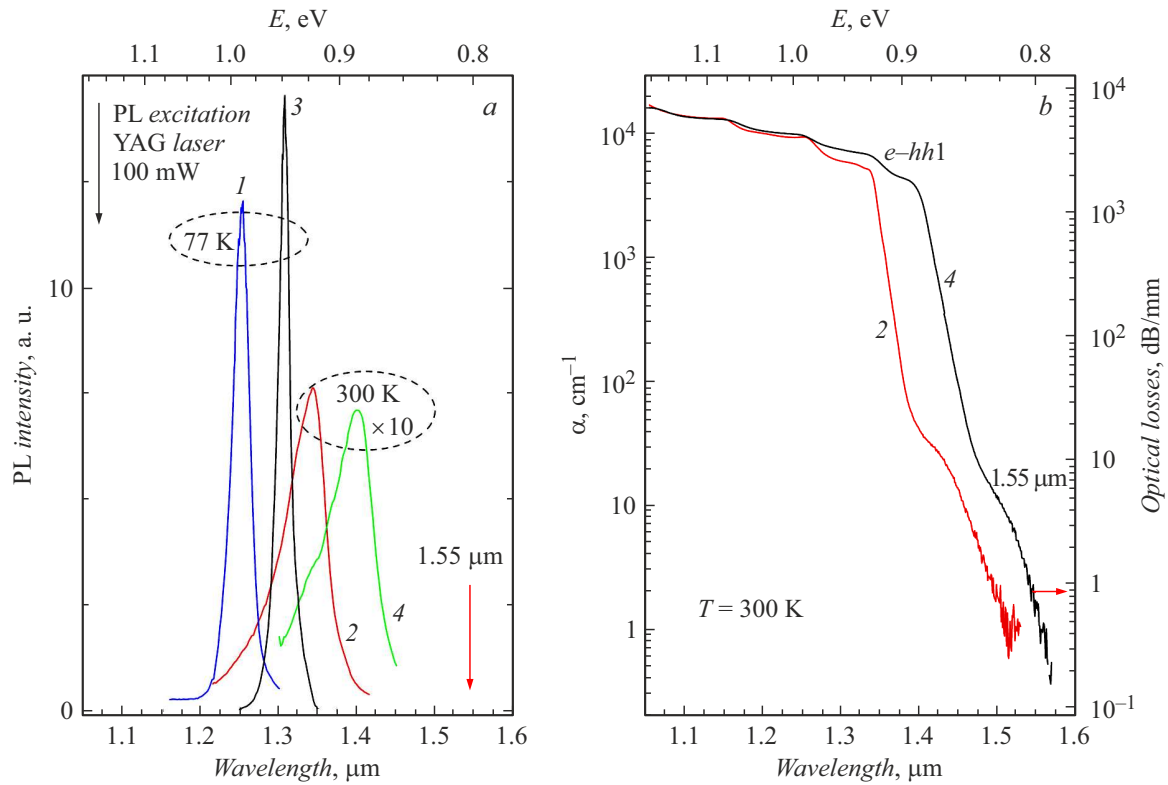


Figure 2. PL spectra (a) and spectral dependence of optical losses (b) of digital InGaAlAs MQWs with the ratio between momolayers InAlAs/InGaAs of 2/6 (1, 2) and 2/8 (3, 4).

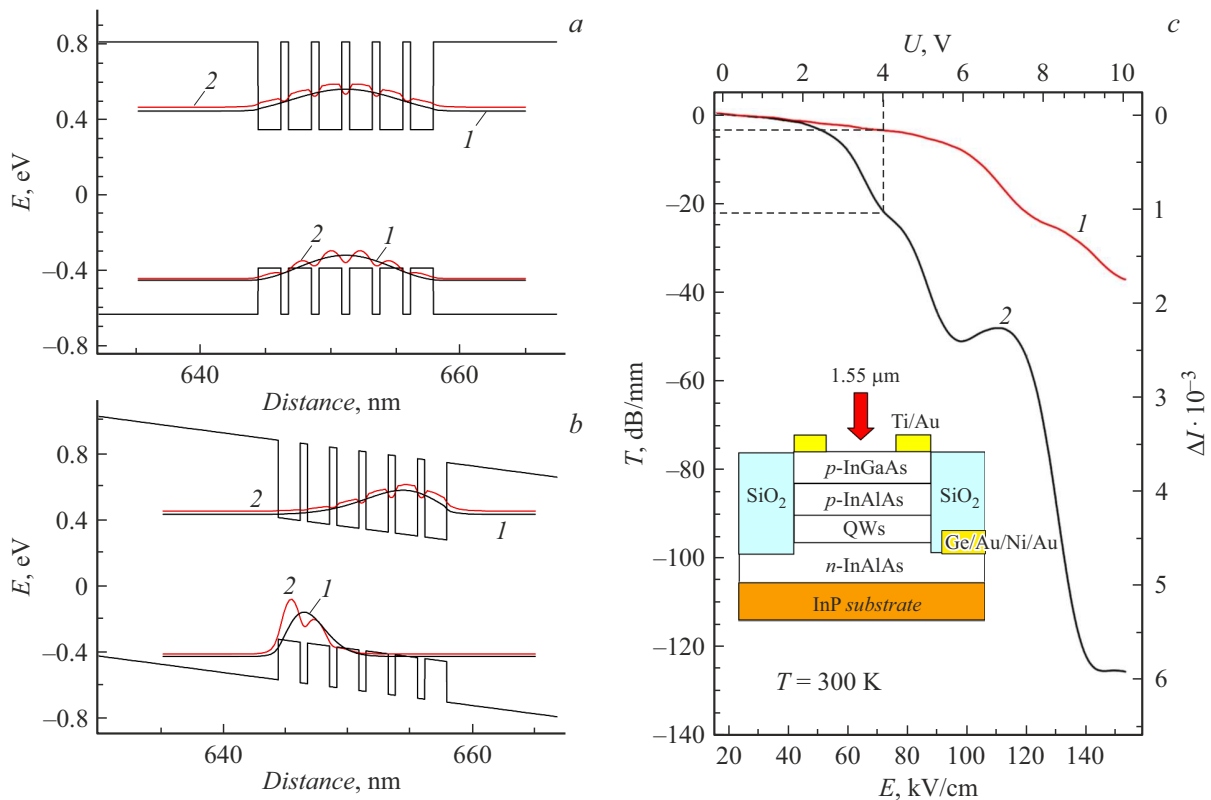


Figure 3. Distribution of the electron and hole wave functions in the absence (a) and in the presence of electric field 100 kV/cm in magnitude (b) for a uniform InGaAlAs/InAlAs QW (1) and digital QW (2). c — the extinction coefficient versus the applied voltage in digital InGaAlAs MQWs with the ratio between monolayers InAlAs/InGaAs of 2/6 (1) and 2/8 (2). The inset presents the experiment geometry. As the source of light 1.55 μm in wavelength, a semiconductor laser with the linewidth of 200 kHz was used.

(at $\Delta I(V) \rightarrow 0$). Then the extinction coefficient is

$$T(V) = 10 \lg(\exp(-\Delta I(V)L/W)) = -10 \lg e \Delta I(V)L/W.$$

As shown by Fig. 3, *c*, the extinction coefficient for MQW with the ratio between monolayers InAlAs/InGaAs of 2/8 does not exceed -20 dB in magnitude at the voltage of 4 V and length of 1 mm. The obtained coefficient value is comparable with literature data on EAM: the typical bias voltage of EAM on the indium–phosphide platform is 1.5–4 V [3–7], while the length of 1 mm at low passive optical losses (Fig. 2, *b*) ensures technological simplicity of the chip packaging and coupling with optic fiber [7]. Therefore, such a HES is well suitable for creating EAM. Notice that the operating bias voltage may be reduced due to a decrease in the ratio between monolayers InAlAs/InGaAs contained in QW and to concomitant approach of the MQW absorption edge to the operating wavelength; however, this effect will be accompanied by enhancement of passive optical losses. In the case of MQW with the ratio between monolayers InAlAs/InGaAs of 2/6, the extinction coefficient does not exceed -3 dB at the voltage of 4 V and length of 1 mm (Fig. 3, *c*), i.e. this HES can be promising for fabricating electro–optical modulators based on the Mach–Zender interferometer which need low optical losses during light propagation.

Thus, this paper demonstrates structural and electro–optical properties of heterostructures with InGaAlAs/InAlAs quantum wells in which the quaternary solution has been obtained by alternating monolayer growth of InAlAs and InGaAs. This method is shown to be promising for creating electro–absorption modulators designed for the wavelength of 1.55 μm .

Acknowledgements

TEM studies were carried out at CCU „Nanostructures“ of ISP RAS SB.

Conflict of interests

The authors declare that they have no conflict of interests.

References

- [1] R. Nagarajan, M. Kato, J. Pleumeekers, P. Evans, S. Corzine, S. Hurtt, A. Dentai, S. Murthy, M. Missey, R. Muthiah, R.A. Salvatore, C. Joyner, R. Schneider, M. Ziari, F. Kish, D. Welch, *IEEE J. Sel. Top. Quantum Electron.*, **16** (5), 1113 (2010). DOI: 10.1109/JSTQE.2009.2037828
- [2] L.M. Augustin, R. Santos, E. den Haan, S. Kleijn, P.J.A. Thijs, S. Latkowski, D. Zhao, W. Yao, J. Bolk, H. Ambrosius, S. Mingaleev, A. Richter, A. Bakker, T. Korthorst, *IEEE J. Sel. Top. Quantum Electron.*, **24** (1), 6100210 (2018). DOI: 10.1109/JSTQE.2017.2720967
- [3] W. Kobayashi, T. Yamanaka, M. Arai, *IEEE Photon. Technol. Lett.*, **21** (18), 1317 (2009). DOI: 10.1109/lpt.2009.2026485
- [4] H. Fukano, T. Yamanaka, M. Tamura, *J. Lightwave Technol.*, **25** (8), 1961 (2007). DOI: 10.1109/JLT.2007.901328
- [5] K. Kim, D.-S. Shin, *J. Opt. Soc. Korea*, **11** (3), 133 (2007). DOI: 10.3807/JOSK.2007.11.3.133
- [6] W.-J. Choi, A.E. Bond, J. Kim, J. Zhang, R. Jambunathan, H. Foulk, S. O'Brien, J. Van Norman, D. Vandegriff, C. Wanamaker, J. Shakespeare, H. Cao, *J. Lightwave Technol.*, **20** (12), 2052 (2002). DOI: 10.1109/JLT.2002.806756
- [7] D. Pasquariello, E.S. Bjorlin, D. Lasoosa, Y.-J. Chiu, J. Piprek, J.E. Bowers, *J. Lightwave Technol.*, **24** (3), 1470 (2006). DOI: 10.1109/JLT.2005.863227
- [8] *Broadband optical modulators: science, technology, and applications*, ed. by A. Chen, E.J. Murphy (CRC Press, 2012).
- [9] D.A.B. Miller, D.S. Chemla, S. Schmitt-Rink, *Phys. Rev. B*, **33** (10), 6976 (1986). DOI: 10.1103/PhysRevB.33.6976
- [10] W.-P. Hong, A. Chin, N. Debbar, J. Hinckley, P.K. Bhattacharya, J. Singh, *J. Vac. Sci. Technol. B*, **5** (3), 800 (1987). DOI: 10.1063/1.100228
- [11] J. Singh, S. Dudley, B. Davies, K.K. Bajaj, *J. Appl. Phys.*, **60** (9), 3167 (1986). DOI: 10.1063/1.337730
- [12] F. Peiró, A. Cornet, J.R. Morante, S.A. Clark, R.H. Williams, *J. Appl. Phys.*, **71** (5), 2470 (1992). DOI: 10.1063/1.351083
- [13] T. Fujii, Y. Nakata, Y. Sugiyama, S. Hiyamizu, *Jpn. J. Appl. Phys.*, **25** (3A), L254 (1986). DOI: 10.1143/JJAP.25.L254
- [14] I. Novikov, A. Nadtochiy, A. Potapov, A. Gladyshev, E. Kolodeznyi, S. Rochas, A. Babichev, V. Andryushkin, D. Denisov, L. Karachinsky, A. Egorov, V. Bougrov, *J. Lumin.*, **239**, 118393 (2021). DOI: 10.1016/J.JLUMIN.2021.118393
- [15] C.L. Chiu, E.Y. Lin, K.Y. Chuang, D.J.Y. Feng, T.S. Lay, *Physica B*, **404** (8-11), 1226 (2009). DOI: 10.1016/j.physb.2008.11.225
- [16] <https://www.nextnano.de>